

# Hubbard model calculations of phase separation in optical lattices

H. Heiselberg\*

*Applied Research, DALO, Lautrupbjerg 1-5, DK-2750 Ballerup, Denmark*

Antiferromagnetic, Mott insulator, d-wave and gossamer superfluid phases are calculated for 2D square lattices from the extended Hubbard (t-J-U) model using the Gutzwiller projection method and renormalized mean field theory. Phase separation between antiferromagnetic and d-wave superfluid phases is found near half filling when the on-site repulsion exceeds  $U \gtrsim 7.3t$ , and coincides with a first order transition in the double occupancy. Phase separation is thus predicted for 2D optical lattices with ultracold Fermi atoms whereas it is inhibited in cuprates by Coulomb frustration which instead may lead to stripes. In a confined optical lattice the resulting density distribution is discontinuous with extended Mott plateau which enhances the antiferromagnetic phase but suppresses the superfluid phase. Observation of Mott insulator, antiferromagnetic, stripe and superfluid phases in density and momentum distributions and correlations is discussed.

PACS numbers: 03.75.Ss, 03.75.Lm, 05.30.Fk, 74.25.Ha, 74.72.-h

Ultra-cold atomic Fermi-gases present a new opportunity to study strongly correlated quantum many-particle systems and to emulate high temperature superconductors (HTc). Optical lattices realize the Hubbard model, when the periodical lattice potential is strong enough so that only the lowest energy band is populated, and interactions, densities, temperatures, etc., can be tuned. Recent experiments with optical lattices have measured momentum distributions and correlations, and have found superfluid phases of Bose and Fermi atoms [1, 2, 3], Mott insulators (MI) [4, 5], and band insulators [6, 7].

Long range Coulomb repulsion between electrons in cuprates prohibits phase separation (PS), which in turn may lead to stripes, whereas PS is allowed for atoms in optical lattices. The various competing phases can be calculated in the 2D t-J-U model within the Gutzwiller projection method and renormalized mean field theory (RMFT). This method approximates the strong correlations and generally agrees well with full variational Monte Carlo calculations [8, 9]. As will be shown below RMFT predicts PS at low doping between an antiferromagnetic (AF) Neel order and a d-wave superfluid (dSF) phase for sufficiently strong onsite repulsion  $U \gtrsim 7.3t$ . The amount of MI, AF and dSF phases, the density distribution and momentum correlations in optical lattices are quite different from what would be expected from HTc cuprates.

The t-J-U model was employed by Laughlin, Zhang and coworkers [9] to study AF, HTc and “gossamer superconductivity” in cuprates and organic superconductors. Both the Hubbard and t-J models are included in the t-J-U Hamiltonian  $H = H_U + H_t + H_s$  or

$$H = U \sum_i \hat{n}_{i\uparrow} \hat{n}_{i\downarrow} - t \sum_{\langle ij \rangle \sigma} \hat{a}_{i\sigma}^\dagger \hat{a}_{j\sigma} + J \sum_{\langle ij \rangle} \mathbf{S}_i \mathbf{S}_j, \quad (1)$$

where  $\hat{a}_{i\sigma}$  is the usual Fermi creation operator,  $\sigma = (\uparrow, \downarrow)$  is the two hyperfine states (e.g.  $(-\frac{9}{2}, -\frac{7}{2})$  for  $^{40}\text{Na}$ ),

$n_{i\sigma} = \hat{a}_{i\sigma}^\dagger \hat{a}_{i\sigma}$  the density,  $\mathbf{S}_i = \sum_{\sigma\sigma'} \hat{a}_{i\sigma}^\dagger \vec{\sigma}_{\sigma\sigma'} \hat{a}_{i\sigma'}$  and  $\langle ij \rangle$  denotes nearest neighbours.  $U$  is the on-site repulsive interaction,  $t$  the nearest-neighbour hopping parameter and  $J$  the spin-spin or super-exchange coupling.

The t-J-U model allows for doubly occupied sites and thereby also MI transitions. As both are observed in optical lattices the t-J-U model is more useful as opposed to the t-J model which allows neither. For large  $U/t$  the t-J-U and Hubbard models reduce to the t-J model with spin-spin coupling  $J = 4t^2/U$  due to virtual hopping. At finite  $J$  and  $U$  the t-J-U model is to some extent double counting with respect to the Hubbard model with  $J = 0$ . However, when RMFT is applied the virtual hopping is suppressed in the Hubbard model which justifies the explicit inclusion of the spin Hamiltonian as done in the t-J-U model. Also, optical “superlattices” provide additional spin-spin interaction [10] and thus realize the unconstrained t-J-U model.

The t-J-U model on a 2D square lattice at zero temperature was studied for various onsite coupling and densities in Refs. [9, 11] but mainly for  $J \simeq 0.3 - 0.5t$ , which is the relevant case for cuprates and organic superconductors. In optical lattices the Hubbard model can be realized with any on-site repulsion by tuning near a Feshbach resonance. For strong onsite repulsion spin-exchange requires  $J = 4t^2/U$  and we will therefore study the t-J-U model with this parameter constraint. However, keeping in mind that for more moderate  $U$  double counting may occur leading to an effective value for  $J$ . We include nearest-neighbour hopping and interactions only and therefore the phase diagram is symmetric around half filling  $n = 1$ , where  $n = N/M$  is the density or filling fraction ( $N$  is the number of electrons or atoms in  $M$  lattices sites).

In the Gutzwiller approximation the trial wave function  $|\psi\rangle = \Pi_i [1 - (1-g)\hat{n}_{i\uparrow}\hat{n}_{i\downarrow}] |\psi_0\rangle$  is a projection of the Hartree-Fock wave function  $\psi_0$ . The variational parameter  $g$  suppresses double occupancy and varies between 0 corresponding to no doubly occupied sites ( $U \rightarrow \infty$ ) and 1 corresponding to no correlations ( $U = 0$ ). In the Gutzwiller projection method the spatial correlations are

\*Electronic address: heiselberg@mil.dk

included only through the renormalization factors  $g_t$  and  $g_s$  defined such that  $\langle H_s \rangle = g_s \langle H_s \rangle_0$  and  $\langle H_t \rangle = g_t \langle H_t \rangle_0$ , where the expectation values are with respect to  $\psi$  and  $\psi_0$  respectively. The renormalization factors are calculated by classical statistics [12, 13]

$$g_s = \left( \frac{n - 2d}{n - 2n_+ n_-} \right)^2, \quad (2)$$

for the spin term and for the hopping term

$$g_t = \sqrt{g_s} \left[ \sqrt{\frac{x_-}{x_+} (x+d)} + \sqrt{\frac{n_-}{n_+} d} \right] \left[ \sqrt{\frac{x_+}{x_-} (x+d)} + \sqrt{\frac{n_+}{n_-} d} \right]. \quad (3)$$

Here  $d$  is the double occupancy,  $n_{\pm} = n/2 \pm m$  the mean up and down occupation numbers for a magnetization  $m$  at each site,  $x = 1 - n$  the doping, and  $x_{\pm} = 1 - n_{\pm}$ . The double occupancy projection factor is given by  $g^2 = d(x+d)/(x_+ x_- n_+ n_- g_s)$ .

The resulting energy is by Gutzwiller projection

$$E = MUd + g_t \langle H_t \rangle_0 + g_s \langle H_s \rangle_0. \quad (4)$$

The RMFT equations for the t-J-U model in the Gutzwiller projection method have been derived [11] in terms of the order parameters for d-wave pairing, hopping average and staggered magnetization (with commensurate nesting vector  $\mathbf{q} = (\pi, \pi)$ , in units where the lattice constant is unity) defined as

$$\Delta_{\langle ij \rangle} = \langle \hat{a}_{i\downarrow} \hat{a}_{j\uparrow} - \hat{a}_{i\uparrow} \hat{a}_{j\downarrow} \rangle_0 = \pm \Delta, \quad (5)$$

$$\chi = \langle \hat{a}_{i\uparrow}^\dagger \hat{a}_{j\downarrow} + \hat{a}_{i\downarrow}^\dagger \hat{a}_{j\uparrow} \rangle_0, \quad (6)$$

$$m = (-1)^i \langle \hat{a}_{i\uparrow}^\dagger \hat{a}_{i\downarrow} + \hat{a}_{i\downarrow}^\dagger \hat{a}_{i\uparrow} \rangle_0 / 2, \quad (7)$$

respectively. The (+/-) in (5) corresponds to a difference between neighbour sites  $\langle ij \rangle$  of one lattice unit in the ( $x/y$ ) direction respectively.

The resulting variational energy is [11]

$$E/M = Ud - \tilde{\mu}x - \frac{1}{2M} \sum_k (E_k^+ + E_k^-) + \frac{3}{4} g_s J (\Delta^2 + \chi^2) + 2g_s J m^2. \quad (8)$$

Here, the AF and dSF couples four band energies  $E_k^{\pm} = \sqrt{(\xi_k \mp \tilde{\mu})^2 + (\Delta_d \eta_k)^2}$  and  $-E_k^{\pm}$ , with  $\xi_k = \sqrt{\epsilon_k^2 + \Delta_{af}^2}$ ,  $\epsilon_k = -(g_t t + 3g_s J \chi / 8) \gamma_k$ ,  $\gamma_k = 2(\cos k_x + \cos k_y)$  and  $\eta_k = 2(\cos k_x - \cos k_y)$ .  $\Delta_d = 3g_s J \Delta / 8$  and  $\Delta_{af} = 2g_s J m$  are the dSF and AF order parameters. The Lagrange multiplier  $\tilde{\mu}$  differs from the chemical potential because the renormalization factors depend on density as will be discussed later.

Varying the free energy  $F(\Delta, \chi, m, d, \tilde{\mu}) = E - \tilde{\mu}N$  with respect to its five parameters leads to the ‘‘gap’’ equations

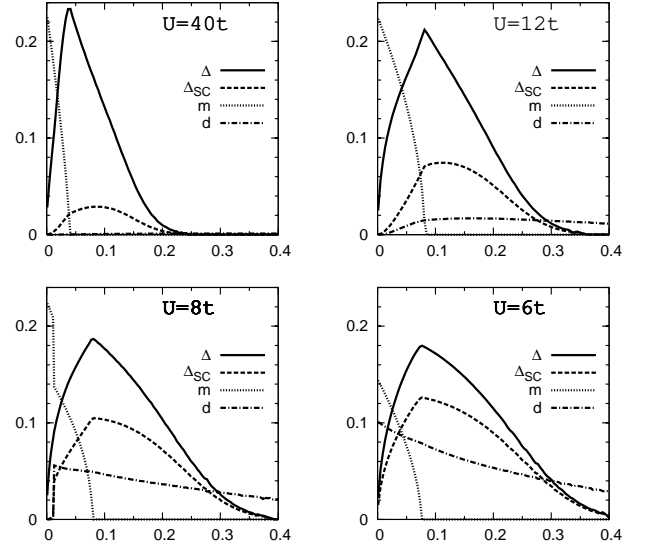


Figure 1: Order parameters vs. doping  $x = 1 - n$  for  $J/t = 4t/U = 0.1, 1/3, 0.5, 2/3$  in RMFT for the 2D t-J-U model.

for the pairing gap, hopping average and density

$$\Delta = \frac{1}{8M} \sum_k \eta_k^2 \Delta_d \left( \frac{1}{E_k^+} + \frac{1}{E_k^-} \right), \quad (9)$$

$$\chi = -\frac{1}{8M} \sum_k \gamma_k \frac{\epsilon_k}{\xi_k} \left( \frac{\xi_k - \tilde{\mu}}{E_k^+} + \frac{\xi_k + \tilde{\mu}}{E_k^-} \right), \quad (10)$$

$$x = \frac{1}{2M} \sum_k \left( \frac{\xi_k - \tilde{\mu}}{E_k^+} - \frac{\xi_k + \tilde{\mu}}{E_k^-} \right). \quad (11)$$

The gap equations that determines the magnetization  $m$  and double occupancy  $d$  [11] are more complicated since the renormalization factors  $g_s$  and  $g_t$  also depend on  $m$  and  $d$ .

The resulting order parameters for the t-J-U model constrained to the Hubbard or t-J model limit  $J = 4t^2/U$  are presented in Fig. 1 for  $U/t = 40, 12, 8$  and  $6$  corresponding to  $J/t = 0.1, 1/3, 0.5$  and  $2/3$  respectively. At half filling ( $x=0$ ) we find a first order phase transition in which the double occupancy jumps from zero to a finite value for  $J \geq 0.55t$  ( $U \leq 7.3t$ ) similar to Refs. [9, 11]. The ground state remains an AF for smaller  $U$  without any dSF. This is in agreement with expectation for the 2D Hubbard model but in contrast to the results for a fixed  $J = t/3$  [11], where the AF vanishes for  $U \geq 7t$  and a dSF appears for  $U \geq 5.3t$  such that a coexisting AF and dSF at half filling (a ‘‘gossamer superfluid’’) exists between  $5.3 \leq U/t \leq 7$ . The reason for this difference traces back to the larger value for  $J = 4t^2/U$  in our calculation which stabilizes the AF phase and destabilizes dSF because the corresponding two order parameters compete. The first order transition in the double occupancy is, however, robust in the sense that it is driven by the on-site repulsion and remains at a critical value  $U \sim 7 - 9t$  even when  $J$  is allowed to vary independently from the  $J = 4t^2/U$

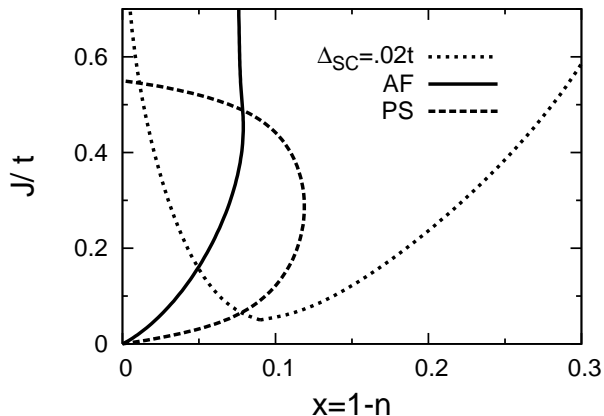


Figure 2: Phase diagram for the t-J-U model under the constraint  $J = 4t^2/U$ . AF and PS occur for  $|x|$  below respective curves. Above dotted curve the dSF gap exceeds  $\Delta_{SC} \geq 0.2t$ . At half filling the first order transition to double occupancy above  $J \geq 0.55t$  is complementary to PS (see text).

constraint. The case  $J = 0.5t$  ( $U = 8t$ ) is close to the critical coupling and we find a transition in  $d$  at low doping as shown in Fig. 1 that also affects the other order parameters  $m$  and  $\Delta_{SC}$ .

The gap depends sensitively on coupling, magnetization and double occupancy. If  $m = d = 0$  the gap equation gives  $\Delta = \chi = \sum_k \sqrt{\cos^2 k_x + \cos^2 k_y} / (2\sqrt{2}M) \simeq 0.339$  at half filling. At low densities the gap equation simplifies because there is no AF order  $\Delta_{af} = 0$ . The gap equation depends on the pairing to quasi-particle energy ratio  $2\Delta_d/\epsilon_{k=0} = V\Delta$ , where  $V \equiv 1/(\chi + 8g_t/3g_sJ) \simeq 3J/4t$  is the effective pairing coupling divided by the bandwidth. Also the Fermi surface becomes circular with Fermi momentum  $k_F = \sqrt{2\pi n}$  and  $\tilde{\mu} = (k_F^2 - 4)(g_t + 3g_sJ\chi/8)$ . The r.h.s. of the gap equation (9) can then be calculated analytically to leading logarithmic order in the effective coupling and to leading orders in the density. The resulting gap becomes

$$\Delta = \frac{1}{V\sqrt{n}} \exp \left[ -\frac{4}{\pi n^2} \left( \frac{1}{V} - c_0 - c_1 n - c_2 n^2 \right) \right]. \quad (12)$$

The higher order corrections in density can be calculated numerically:  $c_0 \simeq 0.27$ ,  $c_1 \simeq 0.57$  and  $c_2 \simeq 0.09$ .

The AF order parameter is defined as the expectation value as in Eq. (5) but for the w.f.  $|\psi\rangle$  instead of  $|\psi\rangle_0$ . It therefore also attains a renormalization factor  $m_{AF} = \sqrt{g_s}m$  [11]. Likewise the dSF order parameter is renormalized  $\Delta_{SC} = g_\Delta\Delta$  with  $g_\Delta = \frac{\sqrt{g_s}}{2} ([\sqrt{\frac{x_-}{x_+}}(x+d) + \sqrt{\frac{n_-}{n_+}}d]^2 + [\sqrt{\frac{x_+}{x_-}}(x+d) + \sqrt{\frac{n_+}{n_-}}d]^2)$ , and is shown in Fig. 1. We expect that the dSF critical temperature is similar.

Since the renormalization factors depend on density the chemical potential  $\mu = dE/dN$  differs from the Lagrange multiplier  $\tilde{\mu}$  by

$$\mu = \tilde{\mu} + \langle H_t \rangle_0 \frac{\partial g_t}{\partial n} + \langle H_s \rangle_0 \frac{\partial g_s}{\partial n}. \quad (13)$$

Near half filling the chemical potential decreases with increasing density in the AF phase i.e. the energy dependence on density is concave. This is unphysical and signals PS to an AF phase at half filling coexisting with a dSF phase at a density  $|x| \lesssim 0.14$  shown in Fig. 2 that is determined by the Maxwell construction. The PS is found to terminate at coupling  $J \simeq 0.55t$  ( $U \simeq 7.3t$ ) where the double occupancy undergoes a first order transition from zero to a finite value. Relaxing the  $J = 4t^2/U$  constraint does not change the phases or PS qualitatively except for gossamer dSF.

Whereas PS is prohibited in cuprates by long range Coulomb repulsion between electrons, PS is permitted for the neutral atoms trapped in optical lattices where it leads to discontinuities in the density distribution  $n(r)$  vs. trap radius  $r$ . For a large number of trapped atoms in a shallow confining potential, the Thomas-Fermi approximation applies (see, e.g. [14]). The total chemical potential is then given by the local chemical potential  $\mu(n) = dE/dN$  and the trap potential, which is on the form  $V_2 r^2$  in most experiments,

$$\mu(n) + V_2 r^2 = \mu(n=0) + V_2 R^2. \quad (14)$$

The sum must be constant over the lattice and can therefore be set to its value at the edge or radius  $R$  of occupied lattice sites, which gives the r.h.s. in (14). The chemical potential for the dilute lattice gas in the 2D Hubbard model is  $\mu(n=0) = -4t$  whereas just below half filling it lies between  $\mu(n=1) = 0$  when  $U = 0$  and  $\mu(n=1) = 4t$  when  $U = \infty$ . Correspondingly the cloud size, when PS or a MI phase appears in the centre, lies between  $R_c \leq R \leq 2R_c$ , where  $R_c = 2\sqrt{t/V_2}$ , and the number of trapped particles  $N = 2\pi \int_0^R n(r)rdr$  is of order  $N_c = \pi R_c^2$ . When more particles are added a MI plateau forms in the centre (see Fig. 3) because the chemical potential has a gap  $\Delta\mu$  at half filling. This gap and the chemical potential above half filling can be found from particle-hole symmetry which implies  $E(-x) = E(x) + MUx$ , such that  $\mu(-x) = U - \mu(x)$ . We find that as  $U$  decreases so does  $\Delta\mu$  but it remains finite even though the double occupancy undergoes a first order transition to a finite value, i.e. the MI remains along with the AF phase. The approximation  $J = 4t^2/U$  is, however, only a valid for large  $U$  and the constrained t-J-U model may not describe the Hubbard model well for large  $J$ . The MI plateau remains in the trap centre until  $N \gtrsim N_c \Delta\mu/t$  corresponding to a trap size  $R \gtrsim \sqrt{\Delta\mu/V_2}$ . Increasing the number of trapped particles further enforces doubly occupied sites and eventually a band insulator with  $n = 2$  in the centre as seen in Fig. 3.

The density distributions and MI plateaus have been measured experimentally for Bose atoms in optical lattices by, e.g., differentiating between singly and doubly occupied sites [2]. A similar technique applied to Fermi atoms might observe the transition in  $d$  at  $U \simeq 7.3t$ . Recently Schneider et al. [5] have measured column densities for Fermi atoms in optical lattices and find evidence for incompressible Mott and band insulator phases. Even

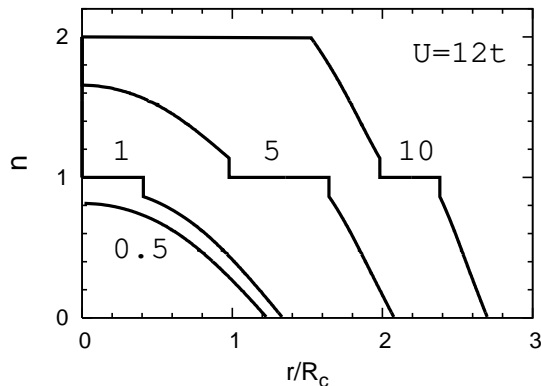


Figure 3: Density distributions of Fermi atoms in an optical lattice confined by a harmonic trap for  $U = 12t$  ( $J = t/3$ ) filled with the number of particles  $N/N_c = 0.5, 1, 5$ , and  $10$ . The density discontinuities from  $n \simeq 1.14$  and  $n \simeq 0.86$  to the MI at  $n = 1$  due to PS between dSF and AF are absent for stripe phases (see text).

lower temperatures are required for observing the AF and dSF phases and the density discontinuities due to PS.

Spin and charge density waves in form of stripes are not included in the above RMFT calculations. Stripes are observed in several cuprates [16] whereas numerical calculations are model dependent. Long range Coulomb frustration can explain why PS is replaced by stripes and an AF phase at very low doping [14] as observed in cuprates. Cold atoms in optical lattices can discriminate between the PS and stripe phases since the latter does not have density discontinuities.

Bragg peaks have been observed for bosons in 3D [2] and 2D [4] optical lattices, and dips for 3D fermions in [7]. The Bragg peaks and dips occur in momentum correlation functions  $C(\mathbf{k}, \mathbf{k}')$  when the relative momentum is  $\mathbf{q} \equiv \mathbf{k} - \mathbf{k}' = \pi(n_x, n_y)$ , where  $n_x, n_y$  are even integers [15]. In an AF phase the periodicity of a given spin is two lattice distances and dips also appears for

odd integers. Just as for the AF phase we can in a stripe phase expect charge and spin correlations as in low energy magnetic neutron scattering [16] at incommensurate  $\mathbf{q} = 2\pi(0, \pm 2x)$  and  $\mathbf{q} = \pi(1, 1 \pm 2x)$  respectively, observed as dips at these wave-numbers. However, because the doping  $x$  varies in the trap, the Bragg dips are distributed over the range of values for  $x$  and are therefore harder to distinguish from the background. If, however, the four stripe periodicity occurs for  $1/8 \leq x \leq 1/4$  as in cuprates, we can expect novel Bragg dips for charge correlations at  $\mathbf{q} = (0, \pm\pi/2)$  and  $\mathbf{q} = (\pm\pi/2, 0)$  and for spin correlations at  $\mathbf{q} = \pi(1, 1 \pm 1/4)$  and  $\mathbf{q} = \pi(1 \pm 1/4, 1)$ . Pairing leads to bunching between opposite momenta  $\mathbf{k} = -\mathbf{k}'$  and s-wave pairing has been observed near the BCS-BEC cross-over [3]. If dSF is enhanced or suppressed by stripes, the bunching due to dSF should be correlated correspondingly with stripe anti-bunching.

3D optical lattices do not have a van Hove singularity at the Fermi surface at half filling as the 2D Hubbard model, and the 2D d-wave symmetry  $\Delta_k \propto (\cos k_x - \cos k_y)$  does not generalize to 3D. Thus we do not expect any significant dSF but by generalizing the RMFT equations to 3D we find MI, AF and PS for the same reasons that they appear in 2D.

In conclusion, t-J-U model RMFT calculations predict phase separation and density discontinuities near half filling in 2D and 3D optical lattices when  $U \gtrsim 7.3t$  coinciding with a first order transition in the double occupancy at half filling. Observation of phase separation would indicate that long range Coulomb frustration is most likely the cause for spin and charge density waves and stripes in cuprates. Contrarily, if no PS is observed but instead a stripe phase near half filling in 2D and probably also 3D optical lattices, then Coulomb frustration is not responsible for stripes in cuprates. In either case optical lattices not only emulate strongly correlated systems, Hubbard type models and can determine the ground state phases such as MI, AF, PS, gossamer and dSF but can even determine more subtle effects from Coulomb frustration.

- 
- [1] T. Stöferle et al., Phys. Rev. Lett. **96**, 030401 (2006).  
[2] S. Fölling et al., Nature **434**, 481 (2005).  
[3] J.K. Chin, D. E. Miller, Y. Liu, C. Stan, W. Setiawan, C. Sanner, K. Xu, W. Ketterle, Nature **443**, 961 (2006).  
[4] I.B. Spielman, W.D. Phillips, and J.V. Porto, Phys. Rev. Lett. **98**, 080404 (2007).  
[5] U. Schneider et al., Science **322**, 1520 (2008)  
[6] M. Köhl, H. Moritz, T. Stöferle, K. Gunter, T. Esslinger, Phys. Rev. Lett. **94**, 080403 (2005).  
[7] T. Rom, Th. Best, D. van Oosten, U. Schneider, S. Foelling, B. Paredes, I. Bloch, Nature **444**, 733 (2006).  
[8] See e.g., B. Edegger, V.N. Muthukumar, C. Gros, Advances in Physics **56**, 927 (2007), and Refs. therein.  
[9] R.B. Laughlin, arXiv:cond-mat/0209269; F.C. Zhang, Phys. Rev. Lett. **90**, 207002 (2003); J.Y. Gan, F.C. Zhang, Z.B. Su, Phys. Rev. B **71**, 014508 (2005).  
[10] A. Klein and D. Jaksch, Phys. Rev. A **73**, 053613 (2006).  
[11] Q. Yuan, F. Yuan, C. S. Ting, Phys. Rev. B **72**, 054504 (2005); F. Yuan, Q. Yuan, C.S. Ting, and T.K. Lee, arXiv:cond-mat/0409596.  
[12] T. Ogawa, K. Kanda, and T. Matsubara, Prog. Theor. Phys. **53**, 614 (1975).  
[13] D. Vollhardt, Rev. Mod. Phys. **56**, 99 (1984).  
[14] H. Heiselberg, Phys. Rev. A **74**, 033608 (2006); cond-mat/0802.0127.  
[15] I. Bloch, J. Dalibard, and W. Zwerger, Rev. Mod. Phys. **80**, 885 (2008); E. Altman, E. Demler, and M.D. Lukin, Phys. Rev. A **70**, 013603 (2004). B.M. Andersen and G.M. Bruun, Phys. Rev. A **76**, 041602(R) (2007)  
[16] J.M. Tranquada et al., Phys. Rev. B **54**, 7489 (1996).